Inorganic Chemistry

Article

pubs.acs.org/IC

Hydrazine-Hydrothermal Synthesis and Characterization of the Two New Quaternary Thioantimonates(III) $BaAgSbS_3$ and $BaAgSbS_3·H_2O$

Chang Liu,[†] Yaying Shen,[†] Peipei Hou,[†] Mingjia Zhi,[†] Chunmei Zhou,[†] Wenxiang Chai,[‡] Jian-Wen Cheng,[§] and Yi Liu*[,†]

[†]State Key Laboratory of Silicon Materials, School of Materials Science and Engineering, Zhejiang University, Hangzhou 310027, People's Republic of China

[‡]College of Materials Science and Engineering, China Jiliang University, Hangzhou 310018, People's Republic of China

[§]Key Laboratory of the Ministry of Education for Advanced Catalysis Materials, Institute of Physical Chemistry, Zhejiang Normal University, Jinhua 321004, People's Republic of China

Supporting Information

ABSTRACT: The two new quaternary thioantimonates(III) $BaAgSbS_3$ (**1**) and $BaAgSbS_3·H_2O$ (**2**) have been synthesized through a hydrazine-hydrothermal method at low temperature. Compound **1** possesses a two-dimensional (2D) layer structure, while compound **2** features a three-dimensional (3D) channel framework. The optical band gaps of **1** and **2** are approximately 2.2 and 2.4 eV, respectively. Our results clearly indicated that the hydrazine-hydrothermal method could offer exciting opportunities for exploring novel multinary chalcogenides with diverse crystal structures and interesting physical properties.

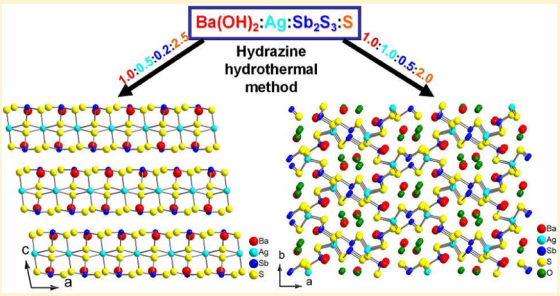

INTRODUCTION

Thioantimonates(III) are attracting more and more interest from scientists due to their diverse structures and potential applications in nonlinear optics, ion exchange, and photocatalysis.[1−3] It is well-known that the physical properties of one material are strongly determined by its structural factors. A special structural feature of thioantimonate(III) chemistry is the presence of the stereochemically active lone electron pairs, which usually play a crucial role in tuning crystal structures and cause Sb(III) centers to have more flexible coordination configurations.[4] In thioantimonates(III), Sb(III) prefers to adopt asymmetric coordination geometries (e.g., $Sb^{III}S_x$ (x = 3−5) as primary building units), which often undergo a variety of self-condensation via vertex and/or edge sharing to form larger structural polyanion units such as diverse chains, layers, and 3D networks.[4a]

On the basis of the coordination features of Sb(III), one can anticipate that the integration of transition metals into thioantimonate(III) networks should produce novel multinary heterometallic thioantimonates(III) with rich structural diversities and significant alterations of physicochemical properties.[1e,4,5] Since Ag(I) ion, one of the late-transition-metal ions, prefers to bond with sulfur, it should be quite easy to introduce the Ag(I) ion into thioantimonate(III) networks to generate new multinary heterometallic thioantimonates(III) with novel structures and integrated properties.[1e,5] In comparison with the large amount of ternary heterometallic thioantimonates(III), only a few quaternary silver thioantimonates(III) containing alkali metals have been reported so far.[5] Additionally, alkaline-earth-metal ions have smaller radii and possess more positive charges in comparison to alkali-metal ions, and therefore, the introduction of alkaline-earth-metal ions into thioantimonate(III) frameworks should generate different crystal structures. Unfortunately, to the best of our knowledge, no quaternary silver thioantimonate(III) containing alkaline-earth-metal ions has been reported so far.

It is well-known that synthetic conditions such as temperature, pressure, solvent, concentration and nature of the starting materials, redox potential, and reaction time have a large effect on the final products. Therefore, exploring a new synthetic strategy to prepare novel multinary thioantimonates(III) is highly desirable and very challenging. Hydro(solvo)thermal methods have been proven to be powerful tools to prepare a variety of multinary thioantimonates(III).[2,3,4a] These methods belong to milder and softer synthetic techniques with the merits of both kinetic and thermodynamic control during the heterogeneous reaction, in which molecular solvents and various amines are typically employed as reaction media and structure-directing agents, respectively.[6] In particular, hydrazine is a basic solvent with strong coordination and reducibility,[7−9] which can simultaneously serve as the reaction medium and structure-directing agent. Although hydrazine has been demonstrated to control the formation of binary or ternary chalcogenides,[1f,7−9] the use of hydrazine as a solvent to grow quaternary chalcogenides is still in its infancy. Herein we report

Received: May 3, 2015
Published: September 2, 2015

DOI: 10.1021/acs.inorgchem.5b00974
Inorg. Chem. 2015, 54, 8931−8936

the successful growth of the two novel quaternary thioantimonates(III) $BaAgSbS_3$ (**1**) and $BaAgSbS_3{\cdot}H_2O$ (**2**) through a hydrazine-hydrothermal method at low temperature. In addition, the syntheses and crystal structures as well as physical properties of these two compounds have been studied in detailed.

EXPERIMENTAL SECTION

Materials and Methods. All of the reagents used for synthesis were of analytical grade and were directly used without further purification. The optical diffuse reflectance spectra were measured at room temperature on a PerkinElmer Lambda 900 UV−vis−NIR spectrometer equipped with an integrating sphere. $BaSO_4$ was used as the reference material, and the polycrystalline samples were ground well before the measurement. The absorption (α/S) data were calculated from the reflectance using the Kubelka−Munk function, $\alpha/S = (1 - R)^2/2R$, in which R is the reflectance at a given wavelength, α is the absorption coefficient, and S is the scattering coefficient.[10] Thermal stability studies were carried out on a TGA Q500 instrument under a flow of nitrogen (30 mL/min) from 30 to 1000 °C at a heating rate of 10 °C/min. The elemental analyses of Ba, Ag, Sb, and S have been examined with the aid of an EDX-equipped JEOL/JSM-6360A SEM instrument. Powder X-ray diffraction data were recorded on a Bruker D8 Advance diffractometer with graphite-monochromated Cu Kα radiation. The operating 2θ angle ranges from 10 to 80°. Simulation of XRD patterns was carried out with the single-crystal data and diffraction-crystal module of the Mercury (Hg) program, version 1.4.2, available free of charge via the Internet at http://www.iucr.org.

Syntheses of $BaAgSbS_3$ (1) and $BaAgSbS_3{\cdot}H_2O$ (2). Compounds **1** and **2** were initially obtained by identical reactions as follows: 1.0 mmol of $Ba(OH)_2$, 0.5 mmol of Ag, 0.2 mmol of Sb_2S_3, 2.5 mmol of S, and 4.0 mL of hydrazine monohydrate (98%) were mixed together and sealed in a 25 mL Teflon-lined stainless autoclave and heated at 160 °C for 7 days. (*Caution! Great care should be taken due to hydrazine monohydrate toxicity and strongly reducing ability.*) The resultant reaction mixtures were washed with ethanol and deionized water, respectively, and a great number of red block-shaped crystals of **1** (Figure S1 in the Supporting Information) (approximately 38% yield based on Ag) and a few yellow plate-shaped crystals of **2** (Figure S2 in the Supporting Information) were obtained. To increase the yield of compound **2**, the ratio of starting reactants has been adjusted as follows: 1.0 mmol of $Ba(OH)_2$, 1.0 mmol of Ag, 0.5 mmol of Sb_2S_3, 2.0 mmol of S, and 4.0 mL of hydrazine monohydrate (98%). A high yield of compound **2** (approximately 50% yield based on Ag) was successfully achieved. Pure phases of these two compounds could be easily obtained by manually picking crystals from the mixtures, and the corresponding XRD patterns are shown in Figures 1 and 2. For compound **1**, the experimental X-ray powder patterns agree well with the simulated patterns. However, for compound **2**, the peak around 11° in 2θ of the simulated powder XRD patterns seems to be very intense in comparison to the experimental peak, which may be due to the anisotropy of crystals of **2** (yellow plate-shaped crystals; Figure S2 in the Supporting Information). The energy-dispersive X-ray analyses gave stoichiometries of these two compounds: Ba:Ag:Sb:S = 1.00:1.02:0.97:2.92 for **1** and Ba:Ag:Sb:S = 1.00:1.03:0.99:2.94 for **2**, which are in agreement with the refined compositions obtained from single-crystal diffraction data (Figures S3 and S4 in the Supporting Information). Both title compounds are reasonably air and water stable for 2 months.

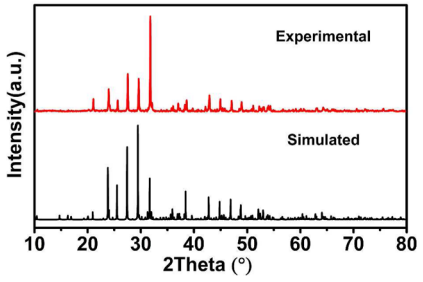

Figure 1. Experimental and simulated XRD patterns of $BaAgSbS_3$ (**1**).

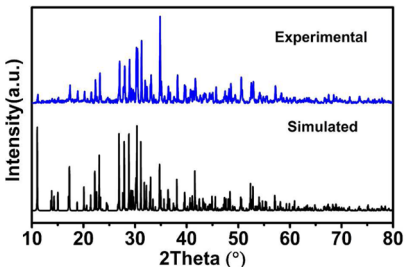

Figure 2. Experimental and simulated XRD patterns of $BaAgSbS_3{\cdot}H_2O$ (**2**).

Single-Crystal X-ray Data Collection and Structure Determination. Suitable single crystals of $BaAgSbS_3$ (**1**) and $BaAgSbS_3{\cdot}H_2O$ (**2**) were mounted on the glass fibers. Diffraction data were collected on an Oxford Xcalibur (Atlas Gemini ultra) diffractometer with graphite-monochromated Mo Kα radiation (λ = 0.71073 Å) at room temperature. The structures were solved by direct methods and refined by full-matrix least-squares fitting on F^2 using the SHELXL-97 software package.[11] All of the atoms were refined with anisotropic displacement parameters. The structures were verified using the ADDSYM algorithm from the program PLATON.[12] Crystal data and refinement details are summarized in Table 1, while the selected bond distances and angles are given in Tables 2 and 3.

Table 1. Crystal Data and Structure Refinement Details for $BaAgSbS_3$ (1) and $BaAgSbS_3{\cdot}H_2O$ (2)

	1	2
empirical formula	$BaAgSbS_3$	$BaAgSbS_3{\cdot}H_2O$
formula wt	463.14	481.16
color	red	yellow
cryst syst	monoclinic	orthorhombic
space group	$C2/c$	$Pna2_1$
a (Å)	9.3675(7)	18.8527(7)
b (Å)	7.9328(5)	8.8232(3)
c (Å)	17.2651(12)	8.6649(3)
α (deg)	90	90
β (deg)	101.734(7)	90
γ (deg)	90	90
V (Å^3)	1256.17(15)	1441.33(9)
Z	8	4
D_{calcd} (g/cm^3)	4.898	4.435
μ (mm^{-1})	14.410	12.577
F(000)	1616	1696
R1, wR2 ($I > 2\sigma(I)$)[a]	0.0360, 0.0978	0.0223, 0.0470
R1, wR2 (all data)[a]	0.0417, 0.1004	0.0237, 0.0477
GOF on F^2	1.267	1.073

[a] $R1 = \sum||F_o| - |F_c||/\sum|F_o|$. $wR2 = [\sum w(F_o^2 - F_c^2)^2/\sum w(F_o^2)^2]^{1/2}$.

RESULTS AND DISCUSSION

Crystal Structure Description. Compound **1**, $BaAgSbS_3$, crystallizes in the monoclinic space group $C2/c$ (No. 15). The structure features a 2D layered $[Ag_2Sb_2S_6]^{4-}$ network, in which the cavities are occupied by Ba^{2+} cations (Figure 3a). Each layered $[Ag_2Sb_2S_6]^{4-}$ network is constructed by infinite $[Ag_2S_4]_n$ chains interconnected by trigonal-pyramidal $Sb(1)S_3$ primary building units via vertex sharing (Figure 3b). The

DOI: 10.1021/acs.inorgchem.5b00974
Inorg. Chem. 2015, 54, 8931−8936

Table 2. Selected Bond Lengths (Å) and Angles (deg) for $BaAgSbS_3$ (1)

Sb(1)−S(1)	2.462(3)	Ag(1)−S(2)	2.509(3)
Sb(1)−S(2)	2.423(3)	Ag(2)−S(1)	2.433(3)
Sb(1)−S(3)	2.421(3)	Ag(1)−Ag(2)	3.095(3)
Ag(1)−S(1)	2.728(3)		
S(2)−Sb(1)−S(1)	97.68(10)	S(2)−Ag(1)−S(2)	166.89(16)
S(3) -Sb(1)−S(1)	101.64(10)	S(2)−Ag(1)−S(1)	98.76(9)
S(3)−Sb(1)−S(2)	98.77(10)	S(2)−Ag(1)−S(1)	87.28(9)
S(1)−Ag(1)−S(1)	125.26(15)	S(1)−Ag(2)−S(1)	161.89(17)

Table 3. Selected Bond Lengths (Å) and Angles (deg) for $BaAgSbS_3·H_2O$ (2)

Sb(1)−S(1)	2.419(2)	Ag(1)−S(2)	2.515(3)
Sb(1)−S(5)	2.431(3)	Ag(1)−S(3)	2.598(3)
Sb(1)−S(6)	2.441(3)	Ag(1)−S(6)	2.642(3)
Sb(2)−S(2)	2.491(2)	Ag(2)−S(1)	2.653(4)
Sb(2)−S(3)	2.439(3)	Ag(2)−S(2)	2.506(3)
Sb(2)−S(4)	2.433(3)	Ag(2)−S(4)	2.582(3)
Ag(1)−S(1)	2.628(4)	Ag(2)−S(5)	2.607(3)
S(1)−Sb(1)−S(5)	99.16(11)	S(2)−Ag(1)−S(6)	113.61(10)
S(1)−Sb(1)−S(6)	97.77(11)	S(3)−Ag(1)−S(1)	94.55(9)
S(5)−Sb(1)−S(6)	97.65(7)	S(3)−Ag(1)−S(6)	106.77(10)
S(3)−Sb(2)−S(2)	98.79(10)	S(2)−Ag(2)−S(1)	113.31(9)
S(4)−Sb(2)−S(2)	99.50(10)	S(2)−Ag(2)−S(4)	123.81(10)
S(4)−Sb(2)−S(3)	96.02(9)	S(2)−Ag(2)−S(5)	114.09(10)
S(1)−Ag(1)−S(6)	98.06(9)	S(4)−Ag(2)−S(1)	95.95(9)
S(2)−Ag(1)−S(1)	122.84(9)	S(4)−Ag(2)−S(5)	108.85(10)
S(2)−Ag(1)−S(3)	117.72(9)	S(5)−Ag(2)−S(1)	95.92(10)

$[Ag_2S_4]_n$ chain is made of the distorted-tetrahedral $Ag(1)S_4$ and bent linearly coordinated $Ag(2)S_2$ units (Figure 3c), which are connected with each other via sharing S(1) atoms along the *a* axis. In this structure, there is only one Sb(1) crystallographic atom, which adopts a distorted-trigonal-pyramidal geometry to coordinate with the three atoms S(1), S(2), and S(3). The distances between Sb(1) and S range from 2.421(3) to 2.462(3) Å, and the S−Sb−S angles are between 97.68(10) and 101.64(10)°. These geometrical parameters of $Sb(1)S_3$ units are comparable to those observed in $[C_4N_2H_{14}][Ag_3Sb_3S_7]$,[13] $[C_6N_4H_{20}][Ag_5Sb_3S_8]$,[14] $[C_2N_2H_9]_2[Ag_2SbS_3]$,[15] and $A_3Ag_9Sb_4S_{12}$ (A = K, Rb, Cs).[5a] Of the two crystallographic Ag(1) and Ag(2) atoms, Ag(1) exhibits a severely distorted tetrahedral coordination with two S(1) atoms (distances 2.728(3) Å and S(1)−Ag(1)−S(1) angles 125.26(15)°) and two S(2) atoms (distances 2.509(3) Å and S(2)−Ag(1)−S(2) angles 166.89(16)°), while Ag(2), however, only coordinates with two S(1) atoms with a bond distance of 2.433(3) Å and adopts approximately linear coordination with S(1)−Ag(2)−S(1) angles of 161.89(17)°. The geometrical parameters of bond distances and angles are comparable to those previously reported for silver sulfides in tetrahedral or linear coordination.[5,13−15] The interchain Ag(1)−Ag(2) distances are 3.095(3) Å, which are longer than those in the Ag metal structure (2.88 Å), suggesting weak d^{10}−d^{10} interactions (less than 3.3 Å).[16] In the structure of **1**, there is only one type of Ba site, which is coordinated with seven S atoms to form an irregular polyhedron, and the Ba−S bonds range from 3.165(3) to 3.369(3) Å, which are comparable to those of $Ba_3Cu_4SbS_6OH$, $BaCuSbS_3$, and $BaCu_2S_2$.[4d] Meanwhile, three types of S atoms adopt different bridging modes: S(1) atoms adopt a μ_3-trigonal geometry to bond one Sb and two Ag atoms and S(2) atoms adopt a μ_2-V shaped mode to link one Sb and one Ag atoms, while S(3) atoms serve as unidentate terminal ligands. From a topological point of view, the 2D layer of **1** can be reduced into a (3,4)-connected network topology (Figure S5 in the Supporting Information), in which the $Sb(1)S_3$ trigonal pyramids act as 3-connected nodes, the Ag(1) ions as 4-connected nodes, and the Ag(2) ions as the linkers.

Interestingly, $KHgSbS_3$, which has been reported by Nagashima et al.,[17] is isostructural with $BaAgSbS_3$. Although both compounds exhibit similar layer structures, a simple comparison suggests that there are two differences between them: (a) $BaAgSbS_3$ was prepared through the hydrazine-hydrothermal method, while $KHgSbS_3$ was synthesized by conventional methods, and (b) due to the different ionic radii and positive charges of Ag^+ and Hg^{2+} ions, both Hg centers in $KHgSbS_3$ adopt a distorted-tetrahedral geometry to coordinate with three S atoms, while in compound **1**, Ag(1) atoms are tetrahedrally coordinated by four S atoms and Ag(2) atoms are nearly linearly linked with two S atoms.

Compound **2**, $BaAgSbS_3·H_2O$, crystallizes in the orthorhombic space group $Pna2_1$ (No. 33) and contains a 3D channeled $[Ag_2Sb_2S_6]^{4-}$ framework with Ba^{2+} cations and water molecules located in the channels (Figure 4a). Although **1** and **2** have the same stoichiometry except for free water molecules in **2**, their structures are totally different. In a view along the *c* axis, the $[Ag_2Sb_2S_6]^{4-}$ channel (Figure 4b) is composed of infinite $[Ag_2SbS_6]_n$ ribbons interconnected by $Sb(1)S_3$ pyramids. Furthermore, the ribbons of $[Ag_2SbS_6]_n$ are constructed by zigzag $[Ag_2S_3]_n$ chains, which are further connected with each other through $Sb(2)S_3$ pyramids (Figure 4c). Meanwhile, the $[Ag_2S_3]_n$ chain is assembled by two vertex-sharing $Ag(1)S_4$ and $Ag(2)S_4$ tetrahedra alternately along the *c* axis. The crystallographic Sb(1) and Sb(2) atoms are both regularly coordinated with three different S atoms at distances from 2.419(2) to 2.491(2) Å in an approximately trigonal pyramidal geometry with S−Sb−S angles between 96.02(9)

DOI: 10.1021/acs.inorgchem.5b00974
Inorg. Chem. 2015, 54, 8931−8936

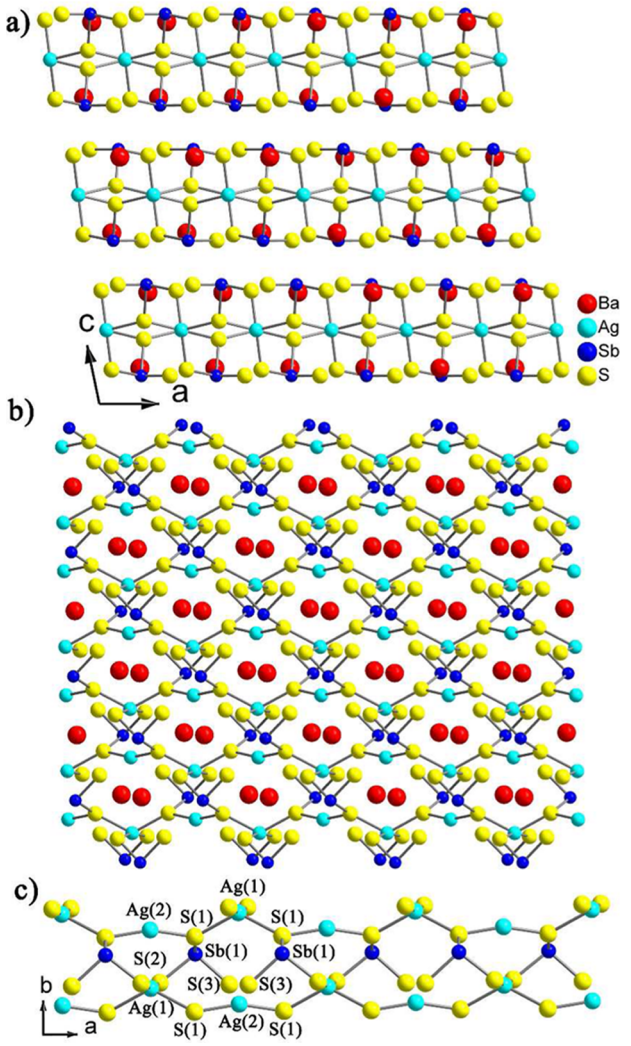

Figure 3. (a) 2D layered structure of **1** along the *b* direction. (b) 2D $[Ag_2Sb_2S_6]^{4-}$ layer of **1**. (c) 1D $[Ag_2S_4]_n$ chains constructed by distorted tetrahedral $Ag(1)S_4$ and bent linear $Ag(2)S_2$ units.

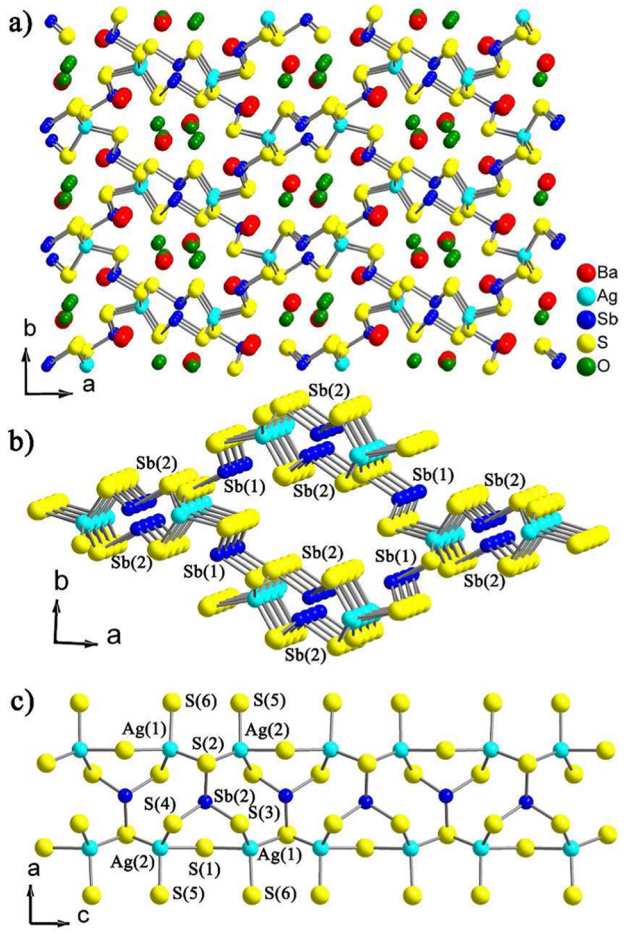

Figure 4. (a) 3D network of **2** along the *c* direction. (b) 3D $[Ag_2Sb_2S_6]^{4-}$ channel constructed by 1D $[Ag_2SbS_6]_n$ ribbons and $Sb(1)S_3$ pyramids. (c) 1D $[Ag_2SbS_6]_n$ ribbon of **2**.

and 99.50(10)°. These SbS_3 primary building units are commonly found in the related structures of thioantimonates(III).[5,13−15,18] Both Ag(1) and Ag(2) exhibit a slightly distorted tetrahedral coordination. All the Ag−S bond distances vary from 2.506(3) to 2.653(4) Å, and S−Ag−S angles are between 94.55(9) and 123.81(10)°, which are comparable to corresponding values in the literature for silver sulfides with tetrahedral coordination.[5,13−15] The intrachain Ag(1)−Ag(2) distances are 3.802(1) Å, which are much longer than that in the Ag metal structure (2.88 Å), suggesting no weak d^{10}−d^{10} interactions.[16] There are two types of coordination environments of Ba atoms in the structure of **2**: Ba(1) and Ba(2). Ba(1) is coordinated with four O atoms and five S atoms to form a complex polyhedron with Ba−O and Ba−S bonds ranging from 2.719(9) to 2.964(10) Å and from 3.165(3) to 3.369(3) Å, respectively, while Ba(2) is solely surrounded by eight S atoms forming an irregular coordination polyhedron with Ba−S bonds ranging from 3.246(3) to 3.630(2) Å. Note that these bond lengths are close to those of $Ba_3Cu_4SbS_6OH$, $BaCuSbS_3$, and $BaCu_2S_2$.[4d] In this structure, six types of S atoms adopt two bridging modes: S(1) and S(2) atoms adopt the distorted μ_3-pyramidal geometries to bond one Sb and two Ag atoms, and the others possess the μ_2-V-shaped modes to link one Ag and one Sb. From a topological point of view, the 3D framework of **2** is a four-connected network (Figure S6 in the Supporting Information), if the Ag ions and SbS_3 primary building units are considered as the four-connected nodes.

To date, many multinary silver thioantimonates(III) have been successfully prepared under solvothermal conditions in the presence of organic amines. Although most of them favor the formation of 2D layered structures, in which the amine molecules are usually aligned perpendicular or parallel to the layers, only $A_3Ag_9Sb_4S_{12}$ (A = K, Rb, Cs) and $BaAgSbS_3{\cdot}H_2O$ show 3D frameworks. This could be a consequence of the different stereochemical effects of organic amine and alkali or alkaline-earth metals. Note that these compounds with 3D structures have totally different structural characteristics. Especially in the structure of $A_3Ag_9Sb_4S_{12}$,[5a] Ag(2) atoms are coordinated with three S atoms to form an approximately trigonal planar geometry and these $Ag(2)S_3$ building units are linked via vertex sharing to form the infinite 1D $[Ag_8S_{12}]^{16-}$ chains. Meanwhile, Ag(1) atoms, which exhibit a tetrahedral coordination, are embedded in the $[Ag_8S_{12}]^{16-}$ chains, resulting the complex 1D $[Ag_9S_{12}]^{15-}$ chains. Furthermore, these infinite $[Ag_9S_{12}]^{15-}$ chains are connected by Sb(1) atoms, which adopt a trigonal-pyramidal coordination, to yield 3D channels in which A cations are located. The structural difference between $BaAgSbS_3{\cdot}H_2O$ and $A_3Ag_9Sb_4S_{12}$ reveals that alkali and alkaline-

DOI: 10.1021/acs.inorgchem.5b00974
Inorg. Chem. 2015, 54, 8931−8936

earth metals have different structure-directing effects on the crystallization of thioantimonates(III).

Thermal Analyses and Optical Properties. The thermal behaviors of **1** and **2** were investigated by TGA under a flow of nitrogen. Compound **1** is approximately stable up to 200 °C without weight loss (Figure 5), while compound **2** could be

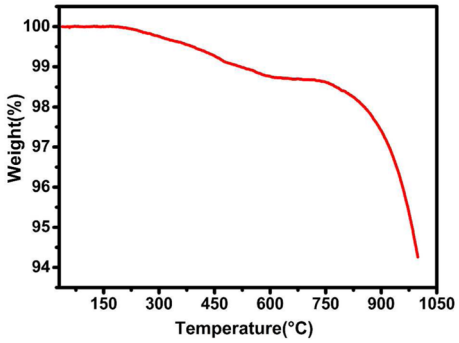

Figure 5. TGA analysis of $BaAgSbS_3$ (**1**).

stable up to 100 °C, and the weight loss (~4.1%) between 100 and 350 °C is close to the complete removal of free water molecules (3.8%) in the compound (Figure 6). The progressive weight loss above 200 °C for **1** and 350 °C for **2** can be attributed to the continuous decomposition and sublimation of S at elevated temperature.

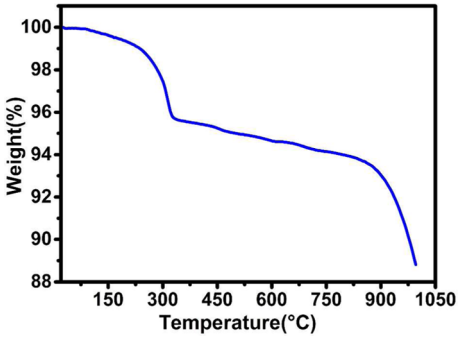

Figure 6. TGA analysis of $BaAgSbS_3·H_2O$ (**2**).

The solid-state UV−visible absorptions for **1** and **2** were measured at room temperature, as shown in Figure 7. The optical absorption spectra of **1** and **2** show the band gaps are

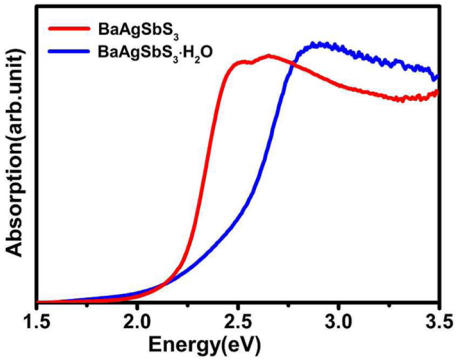

Figure 7. UV−visible absorptions for $BaAgSbS_3$ (**1**) and $BaAgSbS_3·H_2O$ (**2**).

approximately 2.2 and 2.4 eV, which fall in the range of semiconductors and are consistent with the colors of the compounds. The intense absorptions may be due to charge transfer from the primarily sulfur based filled valence band to the mainly antimony and silver based empty conduction band.[5a,b]

CONCLUSION

In summary, two new quaternary thioantimonates(III), $BaAgSbS_3$ (**1**) and $BaAgSbS_3·H_2O$ (**2**), have been successfully synthesized under mild hydrazine-hydrothermal conditions. X-ray single crystal diffraction analysis reveals that compound **1** possesses a 2D layer structure, while compound **2** features a 3D channel framework. The results indicate that the alkaline-earth cation Ba^{2+} can serve as a structure director to prepare new multinary thioantimonates(III). Solid-state optical properties confirmed that compounds **1** and **2** are semiconductors with optical band gaps of around 2.2 and 2.4 eV, respectively. Our success in employing hydrazine as reaction medium to prepare these two quaternary thioantimonates(III) with interesting crystal structures and optical properties could be a promising strategy to approach other novel quaternary chalcogenides at low temperature.

ASSOCIATED CONTENT

Supporting Information

The Supporting Information is available free of charge on the ACS Publications website at DOI: 10.1021/acs.inorgchem.5b00974.

Additional figures giving SEM and EDS information (PDF)

Crystallographic data for **1** and **2** (CIF)

AUTHOR INFORMATION

Corresponding Author

*E-mail for Y.L.: liuyimse@zju.edu.cn.

Notes

The authors declare no competing financial interest.

ACKNOWLEDGMENTS

This work was supported by the National Natural Science Foundation of China (21301153, 21303162, 21471130), the NSF of Zhejiang Province (LY13B010002), and the Foundation of State Key Laboratory of Structural Chemistry (20130001).

REFERENCES

(1) (a) Gandrud, W. B.; Boyd, G. D.; Mcfee, J. H. N. *Appl. Phys. Lett.* **1970**, *16*, 59−61. (b) Zhang, Q. C.; Chung, I.; Jang, J. I.; Ketterson, J. B.; Kanatzidis, M. G. *J. Am. Chem. Soc.* **2009**, *131*, 9896−9897. (c) Chen, M. C.; Li, L. H.; Chen, Y. B.; Chen, L. *J. Am. Chem. Soc.* **2011**, *133*, 4617−4624. (d) Chen, M. C.; Wu, L. M.; Lin, H.; Zhou, L. J.; Chen, L. *J. Am. Chem. Soc.* **2012**, *134*, 6058−6060. (e) Zhao, H. J.; Zhang, Y. F.; Chen, L. *J. Am. Chem. Soc.* **2012**, *134*, 1993−1995. (f) Xiong, W. W.; Zhang, G. D.; Zhang, Q. C. *Inorg. Chem. Front.* **2014**, *1*, 292−301. (g) Xiong, W. W.; Zhang, Q. *Angew. Chem., Int. Ed.* **2015**, DOI: 10.1002/anie.201502277.

(2) (a) Ding, N.; Kanatzidis, M. G. *Nat. Chem.* **2010**, *2*, 187−191. (b) Ding, N.; Kanatzidis, M. G. *Chem. Mater.* **2007**, *19*, 3867−3869. (c) Feng, M. L.; Kong, D. N.; Xie, Z. L.; Huang, X. Y. *Angew. Chem., Int. Ed.* **2008**, *47*, 8623−8626. (d) Wang, K. Y.; Feng, M. L.; Li, J. R.; Huang, X. Y. *J. Mater. Chem. A* **2013**, *1*, 1709−1715. (e) Sheldrick, W. S. *J. Chem. Soc., Dalton Trans.* **2000**, 3041−3052. (f) Dehnen, S.;

DOI: 10.1021/acs.inorgchem.5b00974
Inorg. Chem. 2015, 54, 8931−8936

Melullis, M. *Coord. Chem. Rev.* **2007**, *251*, 1259−1280. (g) Seidlhofer, B.; Pienack, N.; Bensch, W. *Z. Naturforsch., B: J. Chem. Sci.* **2010**, *65*, 937−975.
(3) (a) Feng, M. L.; Hu, C. L.; Wang, K. Y.; Du, C. F.; Huang, X. Y. *CrystEngComm* **2013**, *15*, 5007−5011. (b) Wang, K. Y.; Feng, M. L.; Kong, D. N.; Liang, S. J.; Wu, L.; Huang, X. Y. *CrystEngComm* **2012**, *14*, 90−94. (c) Yue, C. Y.; Lei, X. W.; Liu, R. Q.; Zhang, H. P.; Zhai, X. R.; Li, W. P.; Zhou, M.; Zhao, Z. F.; Ma, Y. X.; Yang, Y. D. *Cryst. Growth Des.* **2014**, *14*, 2411−2421.
(4) (a) Sheldrick, W. S.; Wachhold, M. *Angew. Chem., Int. Ed. Engl.* **1997**, *36*, 206−224. (b) Zhao, H. J.; Zhang, Y. F.; Chen, L. *Inorg. Chem.* **2010**, *49*, 5811−5817. (c) Zhao, H. J.; Zhang, Y. F.; Chen, L. *Inorg. Chem.* **2009**, *48*, 11518−11524. (d) Ma, Z. M.; Weng, F.; Wang, Q. R.; Tang, Q.; Zhang, G. H.; Zheng, C.; Han, R. P. S.; Huang, F. Q. *RSC Adv.* **2014**, *4*, 28937−28940. (e) Wu, Y. D.; Bensch, W. *J. Alloys Compd.* **2012**, *511*, 35−40.
(5) (a) Yao, H. G.; Zhou, P.; Ji, S. H.; Zhang, R. C.; Ji, M.; An, Y. L.; Ning, G. L. *Inorg. Chem.* **2010**, *49*, 1186−1190. (b) Yao, H. G.; Ji, M.; Ji, S. H.; Zhang, R. C.; An, Y. L.; Ning, G. L. *Cryst. Growth Des.* **2009**, *9*, 3821−3824. (c) Wood, P. T.; Schimek, G. K.; Kolis, J. W. *Chem. Mater.* **1996**, *8*, 721−726. (d) Schimek, G. K.; Wood, P. T.; Pennington, W. T.; Kolis, J. W. *J. Solid State Chem.* **1996**, *123*, 277−284. (e) Huang, F. Q.; Ibers, J. A. *J. Solid State Chem.* **2005**, *178*, 212−217.
(6) Xiong, W. W.; Li, P. Z.; Zhou, T. H.; Tok, A. I. Y.; Xu, R.; Zhao, Y. L.; Zhang, Q. C. *Inorg. Chem.* **2013**, *52*, 4148−4150.
(7) (a) Kovalenko, M. V.; Scheele, M.; Talapin, D. V. *Science* **2009**, *324*, 1417−1420. (b) Dolzhnikov, D. S.; Zhang, H.; Jang, J. Y.; Son, J. S.; Panthani, M. G.; Shibata, T.; Chattopadhyay, S.; Talapin, D. V. *Science* **2015**, *347*, 425−428. (c) Son, J. S.; Zhang, H.; Jang, J. Y.; Poudel, B.; Waring, A.; Nally, L.; Talapin, D. V. *Angew. Chem., Int. Ed.* **2014**, *53*, 7466−7470. (d) Huang, X. Y.; Li, J.; Zhang, Y.; Mascarenhas, A. *J. Am. Chem. Soc.* **2003**, *125*, 7049−7055. (e) Li, J. R.; Huang, X. Y. *Dalton Trans.* **2011**, *40*, 4387−4390. (f) Liu, Y.; Kanhere, P. D.; Wong, C. L.; Tian, Y. F.; Feng, Y. H.; Boey, F.; Wu, T.; Chen, H. Y.; White, T. J.; Chen, Z.; Zhang, Q. C. *J. Solid State Chem.* **2010**, *183*, 2644−2649. (g) Liu, Y.; Tian, Y. F.; Wei, F. X.; Ping, M. S. C.; Huang, C. W.; Boey, F.; Kloc, C.; Chen, L.; Wu, T.; Zhang, Q. C. *Inorg. Chem. Commun.* **2011**, *14*, 884−888.
(8) (a) Mitzi, D. B.; Kosbar, L. L.; Murray, C. E.; Copel, M.; Afzali, A. *Nature* **2004**, *428*, 299−303. (b) Mitzi, D. B. *Inorg. Chem.* **2005**, *44*, 7078−7086. (c) Mitzi, D. B. *Inorg. Chem.* **2005**, *44*, 3755−3761. (d) Milliron, D. J.; Mitzi, D. B.; Cope, M.; Murray, C. E. *Chem. Mater.* **2006**, *18*, 587−590. (e) Mitzi, D. B. *Inorg. Chem.* **2007**, *46*, 926−931. (f) Yuan, M.; Dirmyer, M.; Badding, J.; Sen, A.; Dahlberg, M.; Schiffer, P. *Inorg. Chem.* **2007**, *46*, 7238−7240. (g) Yuan, M.; Mitzi, D. B. *Dalton Trans.* **2009**, 6078−6088. (h) Manos, M. J.; Kanatzidis, M. G. *Inorg. Chem.* **2009**, *48*, 4658−4660.
(9) (a) Xiong, W. W.; Miao, J. W.; Ye, K. Q.; Wang, Y.; Liu, B.; Zhang, Q. C. *Angew. Chem., Int. Ed.* **2015**, *54*, 546−550. (b) Xiong, W. W.; Athresh, E. U.; Ng, Y. T.; Ding, J. F.; Wu, T.; Zhang, Q. C. *J. Am. Chem. Soc.* **2013**, *135*, 1256−1259. (c) Nie, L. N.; Xiong, W. W.; Li, P. Z.; Han, J. Y.; Zhang, G. D.; Yin, S. M.; Zhao, Y. L.; Xu, R.; Zhang, Q. C. *J. Solid State Chem.* **2014**, *220*, 118−123. (d) Gao, J. K.; Tay, Q. L.; Li, P. Z.; Xiong, W. W.; Zhao, Y. L.; Chen, Z.; Zhang, Q. C. *Chem. - Asian J.* **2014**, *9*, 131−134.
(10) Kortüm, G. *Reflectance Spectroscopy*; Springer-Verlag: New York, 1969.
(11) Sheldrick, G. M. *Program for Structure Refinement*; University of Göttingen, Göttingen, Germany, 1997.
(12) Spek, A. L. *J. Appl. Crystallogr.* **2003**, *36*, 7−13.
(13) Spetzler, V.; Näther, C.; Bensch, W. *J. Solid State Chem.* **2006**, *179*, 3541−3549.
(14) Powell, A. V.; Thun, J.; Chippindale, A. M. *J. Solid State Chem.* **2005**, *178*, 3414−3419.
(15) Vaqueiro, P.; Chippindale, A. M.; Cowley, A. R.; Powell, A. V. *Inorg. Chem.* **2003**, *42*, 7846−7851.
(16) (a) Jansen, M. *Angew. Chem., Int. Ed. Engl.* **1987**, *26*, 1098−1110. (b) Cui, C. X.; Kertesz, M. *Inorg. Chem.* **1990**, *29*, 2568−2575.
(17) Imafuku, M.; Nakai, I.; Nagashima, K. *Mater. Res. Bull.* **1986**, *21*, 493−501.
(18) (a) Zhou, J.; An, L. T.; Zhang, F. *Inorg. Chem.* **2011**, *50*, 415−417. (b) Zhou, J.; Yin, X. H.; Zhang, F. *Inorg. Chem.* **2010**, *49*, 9671−9676. (c) Zhang, C.; Ji, M.; Ji, S. H.; An, Y. L. *Inorg. Chem.* **2014**, *53*, 4856−4862.

DOI: 10.1021/acs.inorgchem.5b00974
Inorg. Chem. 2015, 54, 8931−8936